

# Osterix functions downstream of anti-Müllerian hormone signaling to regulate Müllerian duct regression

Rachel D. Mullen<sup>a</sup>, Ying Wang<sup>a</sup>, Bin Liu<sup>b</sup>, Emma L. Moore<sup>a</sup>, and Richard R. Behringer<sup>a,1</sup>

<sup>a</sup>Department of Genetics, University of Texas MD Anderson Cancer Center, Houston, TX 77030; and <sup>b</sup>Department of Epigenetics and Molecular Carcinogenesis, University of Texas MD Anderson Cancer Center, Houston, TX 77030

Edited by Patricia K. Donahoe, Pediatric Surgical Research Laboratories, Massachusetts General Hospital, Boston, MA, and approved June 29, 2018 (received for review December 14, 2017)

In mammals, the developing reproductive tract primordium of male and female fetuses consists of the Wolffian duct and the Müllerian duct (MD), two epithelial tube pairs surrounded by mesenchyme. During male development, mesenchyme–epithelia interactions mediate MD regression to prevent its development into a uterus, oviduct, and upper vagina. It is well established that transforming growth factor- $\beta$  family member anti-Müllerian hormone (AMH) secreted from the fetal testis and its type 1 and 2 receptors expressed in MD mesenchyme regulate MD regression. However, little is known about the molecular network regulating downstream actions of AMH signaling. To identify potential AMH-induced genes and regulatory networks controlling MD regression in a global nonbiased manner, we examined transcriptome differences in MD mesenchyme between males (AMH signaling on) and females (AMH signaling off) by RNA-seq analysis of purified fetal MD mesenchymal cells. This analysis found 82 genes up-regulated in males during MD regression and identified *Osterix* (*Osx*)/*Sp7*, a key transcriptional regulator of osteoblast differentiation and bone formation, as a downstream effector of AMH signaling during MD regression. *Osx*/*OSX* was expressed in a male-specific pattern in MD mesenchyme during MD regression. *OSX* expression was lost in mutant males without AMH signaling. In addition, transgenic mice ectopically expressing human AMH in females induced a male pattern of *Osx* expression. Together, these results indicate that AMH signaling is necessary and sufficient for *Osx* expression in the MD mesenchyme. In addition, MD regression was delayed in *Osx*-null males, identifying *Osx* as a factor that regulates MD regression.

*Osterix* | Müllerian duct regression | reproductive tract development | anti-Müllerian hormone | sex differentiation

In mammals, the Wolffian ducts (WDs) differentiate into the male epididymides, vas deferens, and seminal vesicles, whereas the Müllerian ducts (MDs) develop into the female oviducts, uterus, and upper vagina. Reproductive tract differentiation in amniotes is unique because initially both WD and MD are generated in the embryo independent of genetic sex. Sex-specific signaling results in loss of the WD in females and regression of the MD in males (1, 2). MD regression requires transforming growth factor- $\beta$  family member anti-Müllerian hormone (AMH) secreted from the Sertoli cells of the fetal testis and its type 1 and 2 receptors present in MD mesenchyme (3–7). Following AMH binding, AMH type 2 receptor (AMHR2) recruits a type 1 receptor into a heteromeric complex. Within the complex, AMHR2 transphosphorylates and activates the type 1 receptor kinase. This activation results in the phosphorylation of an R-Smad and formation of an R-SMAD/SMAD-4 complex that translocates into the nucleus to transcriptionally activate AMH signaling pathway target genes. AMH type 1 receptors ACVR1 and BMPR1A, and AMH R-Smad effectors (SMAD1, SMAD5, and SMAD8) function redundantly for MD regression and are shared with the bone morphogenetic protein (BMP) pathway (8, 9).

While the upstream components (AMH, type 1 and 2 receptors, and R-Smads) of AMH signaling are well known, the downstream transcriptional effectors of AMH signaling are still largely unidentified. To date, only the WNT pathway effector  $\beta$ -catenin (*Ctnnb1*) has been shown to be required for AMH-induced MD regression in vivo (10). The requirement of *Ctnnb1* for MD regression suggests WNT signaling is important for the downstream actions of AMH during MD regression in males. However, candidate gene approaches have failed to identify an individual WNT, WNT effector, or WNT regulator whose in vivo loss blocks MD regression (10–12).

Because of the limited success of candidate gene approaches in uncovering AMH signaling effectors, in the current study we undertook a nonbiased global approach using next-generation transcriptome sequencing. To elucidate potential gene networks and novel AMH signaling targets, we used RNA-seq analysis of yellow fluorescent protein (YFP)-positive MD mesenchymal cells flow sorted from embryonic day 14.5 (E14.5) *Amhr2*<sup>Cre/+</sup>; *R26R*<sup>Yfp/+</sup> reproductive tracts to identify transcriptome differences between males and females during regression. This analysis identified *Osterix* (*Osx*)/*Sp7* as a downstream effector of AMH signaling during MD

## Significance

In mammals, each embryo forms both male and female reproductive tract progenitor tissues. Anti-Müllerian hormone (AMH) secreted by fetal testes acts on mesenchyme cells adjacent to Müllerian duct (MD) epithelium, the progenitor tissue of female reproductive tract, to induce MD epithelial regression. While AMH and early AMH signaling components are elucidated, downstream gene networks directing this process are largely unknown. A global nonbiased approach using whole-transcriptome sequencing of fetal MD mesenchymal cells identified 82 factors as potential target genes of AMH including *Osterix* (*Osx*). Our findings provide in vivo evidence that *Osx* is an AMH-induced gene that regulates MD regression. Identification of *Osx* may provide key insights into gene-regulatory networks underlying MD regression, male sex differentiation, and mesenchyme–epithelial interactions.

Author contributions: R.D.M. and R.R.B. designed research; R.D.M., Y.W., and E.L.M. performed research; R.D.M., B.L., and R.R.B. analyzed data; and R.D.M. and R.R.B. wrote the paper.

The authors declare no conflict of interest.

This article is a PNAS Direct Submission.

Published under the PNAS license.

Data deposition: The data reported in this paper have been deposited in the Gene Expression Omnibus (GEO) database, <https://www.ncbi.nlm.nih.gov/geo> (accession no. GSE116157).

<sup>1</sup>To whom correspondence should be addressed. Email: rrb@mdanderson.org.

This article contains supporting information online at [www.pnas.org/lookup/suppl/doi:10.1073/pnas.1721793115/-DCSupplemental](http://www.pnas.org/lookup/suppl/doi:10.1073/pnas.1721793115/-DCSupplemental).

Published online July 30, 2018.

regression. Our results indicate that AMH signaling is necessary and sufficient for *Osx* expression in the MD mesenchyme and *Osx* regulates the timing of MD regression.

## Results

**Transcriptome Analysis Identifies Candidate Genes Up-Regulated in Male MD Mesenchyme During Regression.** During embryogenesis, *Amhr2* is expressed in the MD mesenchyme of male and female fetuses, but *Amh* is only expressed in males. Thus, the AMH signaling pathway is only active in male fetuses. To isolate male and female MD mesenchymal cells, *Amhr2-Cre* mice, which express Cre recombinase in the MD mesenchyme and somatic cells of the gonad, were bred to *R26R-YFP* reporter mice (*SI Appendix, Fig. S1*). E14.5 was chosen for this analysis because AMH has been expressed for 2 d in males, there are changes in the MD mesenchyme and MD epithelium, but no breaks or gaps in the MD have occurred. Mice carrying the Cre and YFP alleles were identified by fluorescence, and sex was determined by gross morphology of the gonad using a dissecting microscope. The mesonephros/gonad complex was isolated, and the gonads were removed. Two or more mesonephroi were pooled and digested in trypsin, and the resulting single-cell suspensions were then sorted for YFP<sup>+</sup> cells using FACS (Fig. 1 *A–C*). cDNA libraries were generated from three biological replicates each for male and female. Indexed libraries were pooled and sequenced on the Illumina HiSeq 2000 platform (Fig. 1*D*). Approximately 20 million paired-end 76-bp reads were obtained for each library, of which ~70% mapped to at least one location in the mouse reference genome build NCBI37. Mapped mouse RNA-seq data were then subjected to differential expression analysis, using Cufflinks (13) and DESeq (14). The list of differentially expressed genes was generated based on a false discovery rate of <0.05 and a log2fold change of ≥2. Expression levels (mean of counts normalized to sequencing depth) of differentially up-regulated genes in male and female samples are listed in *SI Appendix, Table S1*. Genes with significant differential expression were then further parsed by removing genes with expression levels below those for *Amh* in males, a gene known to be expressed at low levels in MD mesenchyme (mean counts, <195;

*SI Appendix, Table S1*) (15). These analyses revealed 82 genes that were significantly up-regulated in males versus females during MD regression (Table 1). Ingenuity Pathway Analysis (IPA) predicted both BMP2 and BMP4 as upstream activators (*SI Appendix, Fig. S2*). This is consistent with activation by the AMH signaling pathway because it shares components of the BMP signaling pathway, including type 1 receptors and R-SMADs. In the IPA analysis, we identified the BMP-induced gene, *Osx*, as a male-up-regulated gene (*SI Appendix, Fig. S3*). Our focus on *Osx* was bolstered because it was expressed in the MD of male but not female mouse fetuses (<https://www.gudmap.org/>). This suggested *Osx* as a potential downstream effector of AMH signaling and led us to analyze *Osx* expression and function during MD regression.

**Osterix Is Expressed Only in Male MD Mesenchyme During AMH-Induced MD Regression.** OSTERIX (OSX) is a C2H2-type zinc finger transcription factor first cloned in a screen of C2C12 cells induced by BMP2 to differentiate into osteoblasts. *Osx* is required for osteoblast differentiation and bone formation (16). However, in this study, we identify a role for *Osx* during reproductive tract development. Using in situ hybridization we found that *Osx* transcripts are localized specifically in the male MD mesenchyme at E14.5 (Fig. 2*A* and *B*). To determine whether the OSX protein followed a similar dynamic, we assayed OSX via immunofluorescence and found that OSX is expressed only in male MD mesenchyme at E14.5, indicating a sexually dimorphic expression pattern (Fig. 2*C–E*). This analysis was consistent with the GUDMAP database (<https://www.gudmap.org>) wherein *Osx* expression in the MD has a male-specific pattern (17).

Previously, we generated an *Osx-lacZ* (*Z*)-null allele in mice that originally demonstrated that *Osx* is required for osteoblast differentiation (16). *Osx-lacZ* expresses β-galactosidase from the endogenous *Osx* locus and was used to temporally and spatially map expression of *Osx* during MD regression. Expression of *Osx*<sup>Z/+</sup> begins at around E13.75 in male MD mesenchyme and robust expression throughout the length of the MD is present by E14.5 (Fig. 3*F* and *G*). This temporal expression pattern is consistent with activation of *Osx* expression by the AMH signaling

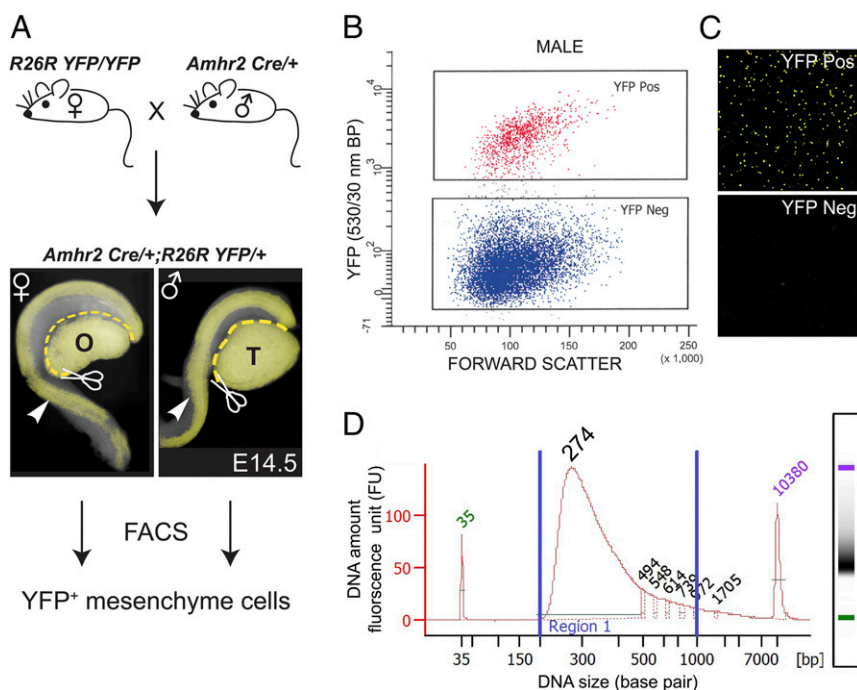


**Fig. 1.** A transcriptome screen for male-specific genes expressed in *Amhr2*-expressing Müllerian duct (MD) mesenchyme. (A) Breeding scheme to isolate *Amhr2*-marked MD mesenchyme cells from E14.5 male and female embryos. The *Amhr2-Cre* allele is expressed in MD mesenchyme cells and somatic cells of the gonad. Mesonephroi containing the MD (arrowheads) and VDs were isolated by removing the gonads. Subsequently, YFP<sup>+</sup> MD mesenchyme cells were isolated by FACS. (B) Representative plot forward scatter versus YFP emission (530/30-nm bandpass filter) from five male *Amhr2*<sup>Cre/+</sup>; *R26R*<sup>YFP/+</sup> mesonephros pairs to isolate YFP<sup>+</sup> cells. (C) Representative confocal image of sorted cell fractions. (D) High-sensitivity DNA chip analysis of index pooled cDNA libraries for RNA-seq. O, ovary; T, testis. (Magnification: A, 40x; C, 200x.)

**Table 1. Genes up-regulated in male MD mesenchyme**

Gene	Logtwo fold change	Gene	Logtwo fold change	Gene	Logtwo fold change	Gene	Logtwo fold change	Gene	Logtwo fold change	Gene	Logtwo fold change
<i>Ankrd63</i>	8.92	<i>Slc22a3</i>	5.24	<i>Dbc1</i>	4.14	<i>Smad6</i>	3.56	<i>Trim9</i>	2.98	<i>Col9a3</i>	2.67
<i>Wif1</i>	8.41	<i>Ednrb</i>	5.10	<i>Ntsr1</i>	4.08	<i>P4ha3</i>	3.43	<i>Fam181b</i>	2.96	<i>Nog</i>	2.57
<i>Syt1</i>	7.57	<i>Syt6</i>	5.09	<i>Enpp1</i>	4.01	<i>Grin3a</i>	3.42	<i>Fam151a</i>	2.96	<i>Bmper</i>	2.55
<i>Galnt5</i>	7.14	<i>Ablim3</i>	4.61	<i>Bean1</i>	4.00	<i>Acot11</i>	3.38	<i>St3gal5</i>	2.93	<i>Stmn2</i>	2.55
<i>Sp6</i>	6.84	<i>Fbxo2</i>	4.59	<i>Pi16</i>	3.94	<i>Galnt14</i>	3.37	<i>Lrrc55</i>	2.92	<i>Hey1</i>	2.54
<i>Dlx5</i>	6.69	<i>Olfm2</i>	4.58	<i>Smad9</i>	3.92	<i>Ntf5</i>	3.23	<i>Id4</i>	2.91	<i>Olfml3</i>	2.54
<i>Gm11532</i>	6.57	<i>Col15a1</i>	4.52	<i>Adam12</i>	3.92	<i>Rap1gap2</i>	3.21	<i>Plcb2</i>	2.86	<i>Rgs2</i>	2.53
<i>Msx2</i>	6.51	<i>Dgkk</i>	4.52	<i>Shisa3</i>	3.82	<i>Slc24a3</i>	3.20	<i>Draxin</i>	2.86	<i>Tagln</i>	2.50
<i>Gata5</i>	6.45	<i>Tac2</i>	4.49	<i>Kazald1</i>	3.80	<i>Gdf10</i>	3.19	<i>Me1</i>	2.82	<i>Gngt2</i>	2.49
<i>Smpd3</i>	5.96	<i>Lor</i>	4.42	<i>Epas1</i>	3.78	<i>Wnk4</i>	3.16	<i>Shisa2</i>	2.78	<i>Bambi</i>	2.47
<i>Ndufa4l2</i>	5.57	<i>H2-T23</i>	4.38	<i>Tgfb1</i>	3.71	<i>Msx1</i>	3.16	<i>Atp1b1</i>	2.76	<i>Pid1</i>	2.43
<i>Aplnr</i>	5.53	<i>Col13a1</i>	4.34	<i>Ntrk3</i>	3.68	<i>Cux2</i>	3.06	<i>Ramp2</i>	2.73	<i>Sox9</i>	2.43
<i>Cadps</i>	5.43	<i>Prss35</i>	4.33	<i>Igfbp7</i>	3.68	<i>Ecm1</i>	3.00	<i>Acta2</i>	2.73		
<i>Ltbp2</i>	5.35	<i>Fgfr3</i>	4.23	<i>Acer2</i>	3.65	<i>Osx</i>	2.99	<i>Unc5b</i>	2.71		

pathway. While *Amh* transcripts are present in the testis as early as E11.5 in mouse, initiation of AMH signaling in the MD follows expression of *Amhr2* in the MD mesenchyme beginning at ~E13.25 (18, 19). No expression is detected in the female reproductive tract at any time points examined (Fig. 3 A–E). In males, *Osx*<sup>Z/+</sup> expression is subsequently lost as the MD regresses (Fig. 3 H–J). The expression patterns of endogenous *OSX* and *Osx-lacZ* suggested that *Osx* expression in the MD mesenchyme is mediated by the AMH signaling pathway.

**AMH Signaling Is Necessary and Sufficient for *OSX/Osterix* Expression in MD Mesenchyme.** To determine whether AMH signaling is required for *Osx* expression in the male MD mesenchyme, we examined *OSX* expression in E14.5 *Amhr2*<sup>Z/Cre</sup> males. *Amhr2*<sup>Z/Cre</sup> is a functional *Amhr2*-null genotype and therefore lacks AMH signaling, leading to female reproductive tract development in mutant males (18, 20). While *OSX* protein can be detected in the MD mesenchyme of wild-type males at E14.5, no detectable *OSX* is present in *Amhr2*<sup>Z/Cre</sup> males (Fig. 4 A and B). The ability of AMH signaling alone to activate *Osx* expression was tested using our *MT-hAMH* transgenic mouse model. The *MT-hAMH* mouse broadly expresses human AMH, causing MD regression in females (5). *Osx-lacZ* is not expressed in E14.5 *Osx*<sup>Z/+</sup> females but is induced in the MD mesenchyme of *Osx*<sup>Z/+</sup>; *MT-hAMH* females (Fig. 4 C–F). These results indicate that activation of the AMH signaling pathway is necessary and sufficient to initiate expression of *Osx/OSX* in the MD mesenchyme during reproductive tract differentiation.

***Osx* Expression Is Downstream of AMH-Effector  $\beta$ -Catenin in MD Mesenchyme.**  $\beta$ -Catenin functions downstream of AMH signaling and is required to regulate MD regression during male sex differentiation (10). However, the downstream molecular targets of  $\beta$ -catenin in the MD mesenchyme are unknown. *Osx* expression is up-regulated by activated  $\beta$ -catenin in osteoblasts, cementoblasts, and long bones (21, 22). In addition, the proximal promoter of *Osx* can be activated by  $\beta$ -catenin in vitro luciferase assays, and  $\beta$ -catenin directly binds the first intron of *Osx* in osteoblasts (21, 23). Therefore, we wanted to determine whether *Osx* is a downstream target of  $\beta$ -catenin in the MD mesenchyme and possibly a contributing factor to the complete block in MD regression observed in males with MD mesenchyme knockout of  $\beta$ -catenin. Reproductive tracts of *Amhr2*<sup>Cre/+</sup>; *Ctnnb1*<sup>flax/flax</sup> male embryos lack expression of  $\beta$ -catenin in the MD mesenchyme and were examined at E14.5 for *OSX* expression by immunofluorescence. *Amhr2*<sup>Cre/+</sup>; *Ctnnb1*<sup>flax/flax</sup> male embryos expressed *OSX* protein in the MD mesenchyme at E14.5 (Fig. 5 A and B).

Loss of  $\beta$ -catenin expression in the MD mesenchyme in *Amhr2*<sup>Cre/+</sup>; *Ctnnb1*<sup>flax/flax</sup> males was confirmed by immunofluorescence (Fig. 5 C and D). Because immunofluorescence is not quantitative, we performed qPCR to detect changes in *Osx* transcript levels in *Amhr2*<sup>Cre/+</sup>; *Ctnnb1*<sup>flax/flax</sup> E14.5 male mesonephroi. These results showed a significant 61% reduction in *Osx* transcript levels in *Amhr2*<sup>Cre/+</sup>; *Ctnnb1*<sup>flax/flax</sup> males in comparison of *Ctnnb1*<sup>flax/flax</sup> controls (Fig. 5E). Specificity of the primers for the *Osx* transcript was confirmed by analysis of *Osx*<sup>Z/Z</sup> and *Osx*<sup>Z/+</sup> E14.5 male mesonephroi. As expected, no *Osx* transcripts were detected in *Osx*<sup>Z/Z</sup> samples and transcripts were reduced by ~50% in *Osx*<sup>Z/+</sup> males (Fig. 5E). Together, the presence of *OSX* protein and reduced *Osx* transcripts in the MD mesenchyme suggests that *Osx* is downstream of *Ctnnb1* but there are other transcriptional activation inputs. Given that we established *Osx* is a downstream target of AMH signaling and AMH-effector  $\beta$ -catenin, we next analyzed the influence of *Osx* loss on MD regression in vivo.

**MD Regression Is Delayed in *Osx*-Null Male Mice.** *Osx*-null mice die at birth with severe skeletal defects (16). However, MD regression is complete in males at the time of birth. To determine whether *Osx* is required for MD regression, we examined *Osx*<sup>Z/Z</sup> embryos at E15.5, E16.5, E17.5, and E18.5. At E15.5, the MD of *Osx*<sup>Z/+</sup> and *Osx*<sup>Z/Z</sup> males are intact. At E15.5, the *Osx*<sup>Z/+</sup> MD is thinner than the *Osx*<sup>Z/Z</sup> MD, indicating a delay in MD regression

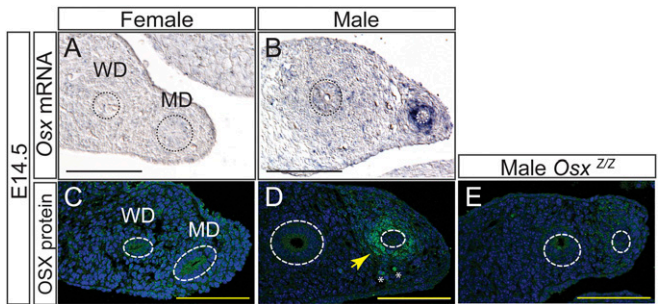


**Fig. 2. Male-specific expression of Osterix in the mouse MD mesenchyme.** (A–D) In situ hybridization for *Osx* transcripts (A and B) and immunofluorescence for *OSX* (C–E) on paraffin sections of mesonephroi at E14.5. MD and WD epithelium outlined with a dashed line. No staining is observed in *Osx*<sup>Z/Z</sup> male controls (E). White asterisk indicates nonspecific autofluorescence. Yellow arrow points to *OSX*-positive MD mesenchyme cells (D). MD, Müllerian duct; WD, Wolffian duct. (Scale bar: 100  $\mu$ m.)



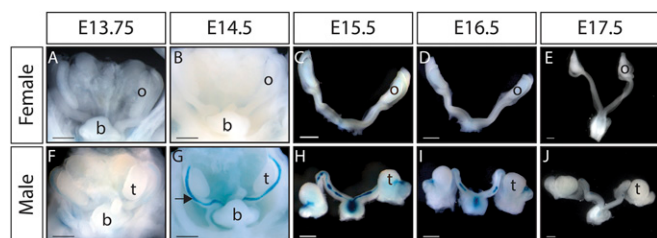


**Fig. 3.** *Osterix-lacZ* (*Osx-Z*) expression is detectable in MD mesenchyme during regression in males but absent in females. (A–J) Whole-mount  $\beta$ -galactosidase staining of *Osx*<sup>Z/+</sup> female and male reproductive tracts. (A–E) No expression is detected in female embryos from E13.75 to E17.5. (F and G) *Osx-lacZ* is expressed in male embryos beginning at E13.75 and by E14.5 is expressed in the mesenchyme throughout the length of the MD. (H–J) As the MD regresses, *Osx-lacZ* expression is also lost. b, bladder; o, ovary; t, testis; (Scale bar: 500  $\mu$ m.)

in the *Osx*<sup>Z/+</sup> males (Fig. 6A and E). At E16.5, the MD of *Osx*<sup>Z/+</sup> males have large gaps. However, the MD of *Osx*<sup>Z/+</sup> males retain longer lengths of intact MD and fewer gaps are observed (Fig. 6B and F). At E17.5, longer MD tissue remnants are observed near the testis in *Osx*<sup>Z/+</sup> males in comparison with *Osx*<sup>Z/+</sup> males (Fig. 6C and G). At E18.5, *Osx*<sup>Z/+</sup> males have a normal pattern of MD regression and the delay in MD regression defects is resolved (Fig. 6D and H). Histological analysis of regressing Müllerian system in *Osx*<sup>Z/+</sup> and *Osx*<sup>Z/+</sup> males showed that the thick stained regions included MD epithelium, whereas the thin stained regions lacked MD epithelium (SI Appendix, Fig. S4). Other developmental delays or growth defects were not evident by gross examination of *Osx*-null males (SI Appendix, Fig. S5). Furthermore, testis morphology and AMH expression were comparable between *Osx*-null mutants and wild type at E13.5 (SI Appendix, Fig. S6). This ~24-h delay in MD regression was observed in all *Osx*-null mutant males examined ( $n = 3$ ). This suggests that *Osx* contributes to MD regression. *Osx* has well-established roles in osteoblast, odontoblast, and cementoblast differentiation (16, 24). However, this is evidence for *Osx* function in sex differentiation.

## Discussion

We report on an AMH-induced mesenchyme gene, *Osx*, as a regulator of MD epithelial regression identified using a global unbiased approach. The identification of *Osx* in this process adds a key link to the gene expression network that may underlie MD regression. During development in skeletal bone and tooth, *Osx* has been demonstrated to be a key mesenchymal factor necessary for cell fate decisions in the differentiation of specialized cells (16, 25). Our study implicates *Osx* as a factor in sex differentiation. In addition to its role in eliminating the MDs in male embryos, AMH is expressed by postnatal ovarian granulosa cells to regulate folliculogenesis (26). Intriguingly, AMH and its type II receptor gene have also been shown to regulate gonadal sex determination in certain species of fishes (27). *Osx* is not expressed in fetal or adult gonads. This suggests that AMH-induced gene regulatory networks are diverse in different tissues with distinct functions. Insights gained into the gene-regulatory networks underlying MD regression, a temporally and spatially defined mesenchyme–epithelial signaling event, may be applied more broadly to further understand mesenchyme–epithelial signaling in other developmental processes and disease.

*Osx* is an important factor in bone homeostasis in adults and has roles in degradation of cartilage matrix by directly transcriptionally activating *matrix metalloproteinase*, *Mmp13* (28). Furthermore, in metastatic breast cancer, modulation of *Osx* levels results in a corresponding change in *MMP-2* promoter activity (29). Two important processes in MD regression are the breakdown of the basement membrane and apoptosis of MD

epithelial cells. Secreted MMPs function to degrade extracellular matrix and also cleave signaling molecules to control multiple cellular processes including differentiation and apoptosis (30). *Mmp2* has been identified as a downstream target of AMH signaling and is expressed in a male-specific pattern in the MD during regression. Knockdown of *Mmp2* using a morpholino and MMP inhibitors block MD regression in in vitro organ culture experiments (31). However, *Mmp2*-null male mice regress the MD, suggesting other MMPs may compensate for loss of MMP-2 (31). Perhaps *Osx* may be contributing to MD regression by regulating MMP levels. However, *Mmp13* is not expressed in our dataset, and there are no differences in *Mmp2* levels in *Osx*-null males compared with controls (SI Appendix, Fig. S7). Thus, it appears that these *Mmp* genes are not OSX targets to mediate MD regression.

The AMH signaling pathway shares type 1 receptors, ACVRI and BMPRI1A, and downstream SMADs with the BMP pathway. This suggests that AMH-induced expression of *Osx* in the reproductive tract may be regulated by similar mechanisms as its regulation by BMP signaling in bone and tooth differentiation. During osteoblast differentiation, BMP signaling induces *Osx* expression by activation of *Runx2* and also via independent mechanisms (32). In our study, *Runx2* transcript is not differentially expressed between male and female E14.5 MD mesenchyme, suggesting in male reproductive tract differentiation *Osx* expression is independent of *Runx2*. In addition to BMP signaling, activated  $\beta$ -CATENIN up-regulates *Osx* expression in osteoblasts, cementoblasts, and long bones (21, 22). In our previous study, we found that  $\beta$ -catenin in the MD mesenchyme is required for AMH-induced regression of the MD. Intriguingly, we found that OSX protein was expressed in  $\beta$ -catenin conditional knockout male mesonephroi but *Osx* transcript levels were significantly reduced compared with controls. Because  $\beta$ -catenin conditional knockout mice have complete retention of the MD and *Osx*-null males only show a delay in MD regression, we interpret this to mean that *Ctnnb1* is upstream of *Osx* but that there are other transcriptional activation inputs. Of note, the chromosomal location of the *Osx* gene is within 88 kb of the *Amhr2* gene, and this linkage is conserved in mammals. This implies the potential for shared enhancer/regulatory elements for MD mesenchyme expression.

Interestingly, Park et al. (12) performed a related study but used microarrays to determine transcript profiles of whole E14.5 mesonephroi from wild-type and *Amhr2* mutant males to identify AMH-induced genes. Our study (MD mesenchymal cells only) and the Park study (whole mesonephroi) resulted in very similar

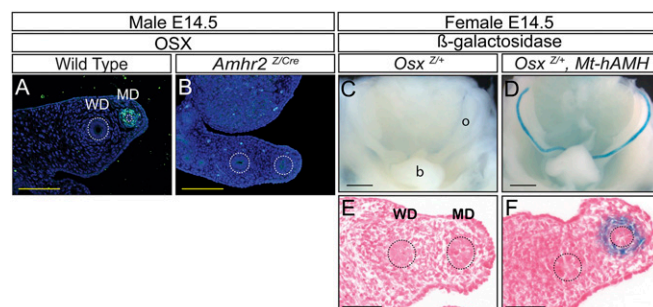


**Fig. 4.** AMH signaling is necessary and sufficient for OSX expression in the MD mesenchyme. (A and B) Immunofluorescence for OSX on paraffin sections of mesonephroi at E14.5. OSX is not expressed in *Amhr2*<sup>Z/Cre</sup> males, indicating AMH signaling is required for OSX expression in the male MD. (C–F)  $\beta$ -Galactosidase staining of *Osx*<sup>Z/+</sup> and *Osx*<sup>Z/+</sup>; *Mt-hAMH* female reproductive tracts. Activation of the AMH signaling pathway in the female reproductive tract is sufficient to induce expression of *Osx-lacZ* in the MD. MD and WD epithelium outlined with a dashed line. b, bladder; MD, Müllerian duct; o, ovary; WD, Wolffian duct. [Scale bars: 100  $\mu$ m (A, B, E, and F); 500  $\mu$ m (C and D).]





assay (Life Technologies). Equal quantities of each indexed library were pooled and sequenced on the Illumina HiSeq 2000 platform to generate paired-end 76-bp reads. Raw data files for the RNA-seq analysis have been deposited in the GEO database with the accession number GSE116157.

**Bioinformatic Analysis of Transcriptomes.** RNA-seq data were mapped to the mouse genome with the bioinformatics tools Tophat and Bowtie using reference genome build NCBIM37 (13). Ensembl annotation for the mouse genome was downloaded from the iGenome website ([support.illumina.com/sequencing/sequencing\\_software/igenome.ilmn](http://support.illumina.com/sequencing/sequencing_software/igenome.ilmn)). Mapped RNA-seq data were then subject to differential expression analysis. Two bioinformatics tools were used for the analysis: Cufflink (13) and DESeq (14). Cufflink uses mapped reads to generate a parsimonious set of transcripts, and then estimates the abundance of the transcripts (41). DESeq utilizes the raw counts of mapped reads as data input and uses the negative binomial distribution model (14). Using both methods, a list of genes with significant differential expression was obtained. To study the possible functions related to the changes of gene expression, pathway analysis was performed using IPA tool from Ingenuity Systems (<https://www.ingenuity.com/>) (SI Appendix, Methods).

**In Situ Hybridization.** Embryos and reproductive tissues from neonates or adults were processed and section in situ hybridization was performed as previously described (10). *Osx* RNA probe was generated from plasmid pBSOxBP containing a 560-bp fragment of mouse *Osx* (*Osx* transcript NM\_133045.8.4 base pairs 106–672) (16).

**X-Gal Staining.** Embryos were collected at stages E13.5–E18.5. Lower body trunks with urogenital tissues were isolated and processed for X-gal staining to visualize lacZ expression as described (18). Following  $\beta$ -galactosidase staining, reproductive tracts were embedded in paraffin, sectioned at 10  $\mu$ m, and counterstained with nuclear fast red and/or eosin Y (Sigma Aldrich).

**Immunofluorescence.** Immunofluorescence was performed as previously described (42). Primary antibodies and dilutions are found in SI Appendix, Table S2. At least three specimens of each genotype were analyzed for each staining.

**qPCR.** Total RNA was extracted from whole mesonephroi using TRI reagent RT-LS (Molecular Research Center) and RNA Clean and Concentrator- 5 kit (Zymo Research). cDNA was generated from 50 ng of total RNA per biological replicate using the SuperScript II reverse transcriptase (RT) with supplied oligo(dT)<sub>12–18</sub> primer (Invitrogen). qPCR was performed on cDNA using a 7900HT Thermocycler (Applied Biosystems) and iTAQ hotstart SYBR Green master mix (Bio-Rad). The fold change of the  $\Delta$ CT normalized to *Actb* was used for analysis ( $2^{-\Delta\Delta C_t}$  method). *P* values and statistical significance were determined by either ANOVA followed by Tukey's post hoc analysis (three experimental groups of data) or by Welch's paired *t* test (two experimental groups of data) using GraphPad Prism, version 7.00 for Windows (GraphPad Software; [www.graphpad.com](http://www.graphpad.com)). Threshold *P* value was <0.05. For primer sequences, see SI Appendix, Table S3.

**ACKNOWLEDGMENTS.** We thank Swathi Arur, Erin Lopez, Zer Vue, Shuo-Ting Yen, and Alejandro Elder Ontiveros for helpful discussions. pBSOxBP and OSX antibody were kindly provided by Benoit de Crombrughe. We acknowledge Dr. Paulucci-Holthausen at the Department of Genetics Microscopy Facility for training and support. This work was supported by NIH Grant HD030284 and the Ben F. Love Endowment (to R.R.B.). R.D.M. was supported by NIH T32 Grant CA009299 and a postdoctoral fellowship from Center for Stem Cell and Developmental Biology at University of Texas MD Anderson Cancer Center. We acknowledge NIH Shared Instrumentation Grant (1S10OD024976-01) for supporting the confocal microscope. Veterinary resources, flow cytometry, and DNA sequencing were supported by NIH Grant CA16672.

- Zhao F, et al. (2017) Elimination of the male reproductive tract in the female embryo is promoted by COUP-TFI in mice. *Science* 357:717–720.
- Mullen RD, Behringer RR (2014) Molecular genetics of Müllerian duct formation, regression and differentiation. *Sex Dev* 8:281–296.
- Josso N, et al. (1993) Anti-Müllerian hormone: The Jost factor. *Recent Prog Horm Res* 48:1–59.
- Behringer RR (1994) The in vivo roles of Müllerian-inhibiting substance. *Curr Top Dev Biol* 29:171–187.
- Mishina Y, et al. (1996) Genetic analysis of the Müllerian-inhibiting substance signal transduction pathway in mammalian sexual differentiation. *Genes Dev* 10:2577–2587.
- Picard JY, Cate RL, Racine C, Josso N (2017) The persistent Müllerian duct syndrome: An update based upon a personal experience of 157 cases. *Sex Dev* 11:109–125.
- Behringer RR, Cate RL, Froelich GJ, Palmiter RD, Brinster RL (1990) Abnormal sexual development in transgenic mice chronically expressing Müllerian inhibiting substance. *Nature* 345:167–170.
- Jamin SP, Arango NA, Mishina Y, Behringer RR (2002) Genetic studies of MIS signalling in sexual development. *Novartis Found Symp* 244:157–164; discussion 164–168, 203–206, 253–257.
- Orvis GD, et al. (2008) Functional redundancy of TGF-beta family type I receptors and receptor-Smads in mediating anti-Müllerian hormone-induced Müllerian duct regression in the mouse. *Biol Reprod* 78:994–1001.
- Kobayashi A, et al. (2011)  $\beta$ -Catenin is essential for Müllerian duct regression during male sexual differentiation. *Development* 138:1967–1975.
- Cox S, et al. (2006) Sexually dimorphic expression of secreted frizzled-related (SFRP) genes in the developing mouse Müllerian duct. *Mol Reprod Dev* 73:1008–1016.
- Park JH, et al. (2014) Induction of WNT inhibitory factor 1 expression by Müllerian inhibiting substance/antiMüllerian hormone in the Müllerian duct mesenchyme is linked to Müllerian duct regression. *Dev Biol* 386:227–236.
- Trapnell C, et al. (2012) Differential gene and transcript expression analysis of RNA-seq experiments with TopHat and Cufflinks. *Nat Protoc* 7:562–578.
- Anders S, Huber W (2010) Differential expression analysis for sequence count data. *Genome Biol* 11:R106.
- Münsterberg A, Lovell-Badge R (1991) Expression of the mouse anti-Müllerian hormone gene suggests a role in both male and female sexual differentiation. *Development* 113:613–624.
- Nakashima K, et al. (2002) The novel zinc finger-containing transcription factor Osterix is required for osteoblast differentiation and bone formation. *Cell* 108:17–29.
- Harding SD, et al. (2011) The GUDMAP database—an online resource for genitourinary research. *Development* 138:2845–2853.
- Arango NA, et al. (2008) A mesenchymal perspective of Müllerian duct differentiation and regression in *Amhr2*-lacZ mice. *Mol Reprod Dev* 75:1154–1162.
- Hacker A, Capel B, Goodfellow P, Lovell-Badge R (1995) Expression of *Sry*, the mouse sex determining gene. *Development* 121:1603–1614.
- Jamin SP, Arango NA, Mishina Y, Hanks MC, Behringer RR (2002) Requirement of *Bmpr1a* for Müllerian duct regression during male sexual development. *Nat Genet* 32:408–410.
- Bao Q, et al. (2017) Constitutive  $\beta$ -catenin activation in osteoblasts impairs terminal osteoblast differentiation and bone quality. *Exp Cell Res* 350:123–131.
- Choi H, et al. (2017) A reciprocal interaction between  $\beta$ -catenin and Osterix in cementogenesis. *Sci Rep* 7:8160.
- Felber K, Elks PM, Lecca M, Roehl HH (2015) Expression of Osterix is regulated by FGF and Wnt/ $\beta$ -catenin signalling during osteoblast differentiation. *PLoS One* 10:e0144982.
- He YD, et al. (2016) Site-specific function and regulation of Osterix in tooth root formation. *Int Endod J* 49:1124–1131.
- Takahashi A, Ono N, Ono W (2017) The fate of Osterix-expressing mesenchymal cells in dental root formation and maintenance. *Orthod Craniofac Res* 20:39–43.
- Durlinger AL, et al. (1999) Control of primordial follicle recruitment by anti-Müllerian hormone in the mouse ovary. *Endocrinology* 140:5789–5796.
- Pan Q, et al. (2016) Vertebrate sex-determining genes play musical chairs. *C R Biol* 339:258–262.
- Zhang C, Tang W, Li Y (2012) Matrix metalloproteinase 13 (MMP13) is a direct target of osteoblast-specific transcription factor osterix (Ox) in osteoblasts. *PLoS One* 7:e50525.
- Dai QS, et al. (2015) Osterix transcriptional factor is involved in the metastasis of human breast cancers. *Oncol Lett* 10:1870–1874.
- Nagase H, Visse R, Murphy G (2006) Structure and function of matrix metalloproteinases and TIMPs. *Cardiovasc Res* 69:562–573.
- Roberts LM, Visser JA, Ingraham HA (2002) Involvement of a matrix metalloproteinase in MIS-induced cell death during urogenital development. *Development* 129:1487–1496.
- Matsubara T, et al. (2008) BMP2 regulates Osterix through *Msx2* and *Runx2* during osteoblast differentiation. *J Biol Chem* 283:29119–29125.
- Migone FF, et al. (2017) Overactivation of hedgehog signaling in the developing Müllerian duct interferes with duct regression in males and causes subfertility. *Reproduction* 153:481–492.
- Arango NA, Lovell-Badge R, Behringer RR (1999) Targeted mutagenesis of the endogenous mouse *Mis* gene promoter: In vivo definition of genetic pathways of vertebrate sexual development. *Cell* 99:409–419.
- Warr N, et al. (2009) *Sfrp1* and *Sfrp2* are required for normal male sexual development in mice. *Dev Biol* 326:273–284.
- Petit FG, Deng C, Jamin SP (2016) Partial Müllerian duct retention in *Smad4* conditional mutant male mice. *Int J Biol Sci* 12:667–676.
- Tanwar PS, et al. (2010) Focal Müllerian duct retention in male mice with constitutively activated beta-catenin expression in the Müllerian duct mesenchyme. *Proc Natl Acad Sci USA* 107:16142–16147.
- Srinivas S, et al. (2001) Cre reporter strains produced by targeted insertion of EYFP and ECFP into the ROSA26 locus. *BMC Dev Biol* 1:4.
- Braut V, et al. (2001) Inactivation of the beta-catenin gene by Wnt1-Cre-mediated deletion results in dramatic brain malformation and failure of craniofacial development. *Development* 128:1253–1264.
- National Research Council (2011) *Guide for the Care and Use of Laboratory Animals* (National Academies Press, Washington, DC), 8th Ed.
- Trapnell C, et al. (2010) Transcript assembly and quantification by RNA-Seq reveals unannotated transcripts and isoform switching during cell differentiation. *Nat Biotechnol* 28:511–515.
- Stewart CA, et al. (2013) CTNNB1 in mesenchyme regulates epithelial cell differentiation during Müllerian duct and postnatal uterine development. *Mol Endocrinol* 27:1442–1454.